Published in final edited form as:
Free Radic Biol Med. 2009 September 1; 47(5): 568–576. doi:10.1016/j.freeradbiomed.2009.05.023.

Characterization of Novel Radicals from COX-Catalyzed Arachidonic Acid Peroxidation

Qingfeng Yu[a,b], **Preeti Purwaha**[b], **Kunyi Ni**[a], **Chengwen Sun**[b], **Sanku Mallik**[b], and **Steven Y. Qian**[b,*]

[a]Department of Analytical Chemistry, China Pharmaceutical University, Nanjing, 210009, China

[b]Department of Pharmaceutical Sciences, College of Pharmacy, Nursing, and Allied Sciences, North Dakota State University, Fargo, ND, 58105, USA

Abstract

The peroxidation of arachidonic acid (AA) catalyzed by cyclooxygenase (COX) is a well known free radical-mediated process that forms many bioactive products. Due to a lack of appropriate methodologies, however, no comprehensive structural evidence has been found previously for the formation of COX-mediated and AA-derived free radicals. Here we have used a combination of LC/ESR and LC/MS with a spin trap, α-[4-pyridyl-1-oxide]-N-*tert*-butyl nitrone (POBN), to characterize the carbon-centered radicals formed from COX-catalyzed AA peroxidation *in vitro*, including cellular peroxidation in human prostate cancer cells (PC-3). Three types of radicals with numerous isomers were trapped by POBN as ESR-active peaks and MS-active ions of m/z 296, m/z 448, and m/z 548, all stemming from PGF_2-type alkoxyl radicals. One of these was a novel radical centered on the carbon-carbon double bond nearest the PGF ring, caused by an unusual β-scission of PGF_2-type alkoxyl radicals. The complementary non-radical product was 1-hexanol, another novel β-scission product, instead of the more common aldehyde. The characterization of these novel products formed from *in vitro* peroxidation provides a new mechanistic insight into COX-catalyzed AA peroxidation in cancer biology.

Keywords

COX-catalyzed AA peroxidation; Electron Spin Resonance (ESR); ESR Spin Trapping; Free radicals; LC/ESR and LC/MS combination; PC-3 cellular peroxidation

Introduction

Cyclooxygenase (COX) has two isomers, COX-1 and COX-2, that metabolize polyunsaturated fatty acids (PUFAs) such as arachidonic acid (AA) to form prostaglandins (PGs); PGs are important lipid mediators in the response of tissues to oxidative stress, injuries, and inflammation [1]. Unlike COX-1, which is constitutively expressed in most mammalian tissues, the inducible form COX-2 has a more restricted tissue distribution and can be induced

*Corresponding Author: Steven Y. Qian, Ph.D., Department of Pharmaceutical Sciences, College of Pharmacy, Nursing, and Allied Sciences, North Dakota State University, NDSU Dept # 2665, P.O. Box 6050, Fargo, ND 58108-6050, USA, Tel: (701) 231-8511, Fax: (701) 231-8333, E-mail: E-mail: steven.qian@ndsu.edu.

by numerous physiological or pathological stimuli [2-3]. Aberrant or increased expression of COX-2 has been found in a variety of cancers [4-8].

COX is a bi-functional enzyme that synthesizes PGs in two steps: 1) its prostaglandin H synthase activity incorporates two oxygen molecules into AA to generate PGG_2 [9], and 2) its peroxidase activity [10-11], generally coupled with a reducing agent, reduces PGG_2 to form PGH_2, which can be further converted to a second series of PGs (PGD_2, PGE_2, and PGF_2, Reaction 1).

COX-catalyzed peroxidation of PUFAs such as AA is a well known radical-mediated process [12-13]. Spin-trapped free radicals have been studied using an ESR spin trapping technique and COX enzyme reconstituted with heme or Mn^{2+} protoporphyrin IX [14]; radicals were proposed to form before oxygen is incorporated into AA. However, due to the lack of more comprehensive methodologies, there has previously been no direct evidence to delineate the types, structures, and numbers of COX-mediated free radicals, greatly restricting our understanding of the role of free radicals in COX-related bioactivities.

In this study, we have used a combination of LC/ESR and LC/MS to identify and characterize the carbon-centered free radicals formed from COX-catalyzed AA peroxidation *in vitro* in the presence of POBN. Our results demonstrate that three types of spin trapped carbon-centered radicals are formed from either β-scission or structural rearrangement of PGF_2-type alkoxyl radicals. Unlike the radical reaction we observed in lipoxygenase (LOX)-catalyzed peroxidation of many types of PUFAs [15-18], a special β-scission during COX-catalyzed AA peroxidation leads to formation of free radicals centered on the C=C bond nearest the PGF ring and formation of a novel non-radical product, 1-hexanol, rather than an aldehyde (a common β-scission product). The characterization of these novel products formed from peroxidation *in vitro*, including cellular peroxidation of a human prostate cancer cell line (PC-3), improves our knowledge of COX-mediated peroxidation and will assist in further studying of the role of COX peroxidation in cancer biology.

Materials and Methods

Reagents

Ethyl alcohol, ferrous ammonium sulfate, glacial acetic acid (HOAc), 1-hexanol, hydroquinone, porcine hematin, and phenol were purchased from Sigma Chemical Co. (St. Louis, MO). Tris-(hydroxymethyl)-aminomethane (Tris-base) and acetonitrile (ACN, HPLC grade) were obtained from Mallinckrodt Baker Inc. (Phillipsburg, NJ), while water (H_2O, LC-MS grade) was purchased from EMD Chemicals Inc. (Gibbstown, NJ). COX-1 and COX-2 enzymes (ovine) and deuterated AA (AA-D_8) were purchased from Cayman Chemical (Ann Arbor, MI), while AA was obtained from Nu-Chek-Prep Inc. (Elysian, MN). Chelex 100 (200-400 mesh sodium form) was bought from Bio-Rad Laboratories Inc. (Hercules, CA). High purity POBN was purchased from Alexis Biochemicals (San Diego, CA), while deuterated POBN (D_9-POBN) was obtained from CDN Isotopes Inc. (Pointe-Claire, QC, Canada). The human prostate cancer cell line PC-3 was purchased from American Type Culture Collection (ATCC, Manassas VA), while RPMI 1640 medium, fetal bovine serum (FBS), and trysin-EDTA were purchased from GIBCO BRL (Grand Island, NY).

Reaction Conditions

The reactions of COX catalysis of AA were performed in 0.1 M (pH 8.0) “metal-free” Tris-Cl buffer solutions. Metal ions in the Tris-Cl buffer solution were chelated by treatment with Chelex 100 resin to provide a virtually metal-free buffer solution, which passed an ascorbic acid test [19]. The reaction mixture containing 5 Kunit/mL COX enzyme, 100 mM POBN, and

50 μM hematin in Tris-Cl buffer (pH 8.0) was pre-incubated for 5 minutes at 37°C and 600 rpm on a Thermo-Shaker (Boekel Scientific, Feasterville, PA). Five mM reducing agent, *e.g.* phenol or hydroquinone, and 2 mM AA (in ethanol) were then added to start the reaction. This complete reaction mixture (~1% ethanol, *v/v*, from an AA stock solution) was incubated at 37° C and 600 rpm on a Thermo-Shaker in the absence of light. After a 30 min incubation, the COX-catalyzed peroxidation was directly analyzed by off-line ESR or immediately stopped by mixing with ACN for the analysis of on-line LC/ESR and LC/MS as described elsewhere [17-18]. Free radicals from cellular COX-mediated peroxidation were generated with PC-3 cells grown in RPMI 1640 medium supplemented with 10% FBS in an incubator containing a humidified atmosphere of 5% CO_2 at 37°C. At 80~90% confluence, the cells were trypsinized, harvested, and suspended in phosphate buffer saline (PBS) at ~10^7 cells/mL. POBN and AA were then added to the cell suspension (final concentrations of 20 mM and 0.5 mM, respectively) to start the AA peroxidation and POBN spin trapping reaction. After a 30-min incubation, the PC-3 cell suspension was used to directly measure radical formation *via* off-line ESR or was processed for LC/ESR and LC/MS analysis with enzyme denaturation (mixing with 1:1 ACN, *v/v*, to stop the cellular peroxidation), supernatant collection (centrifuging the ACN-suspension mixture at 10,000 rpm for 10 min), and sample condensation (in Vacufuge™ 5301 concentrator to evaporate the added ACN) [17-18].

Off-Line ESR Measurements

The COX reaction mixture and PBS-cell suspensions were used directly for off-line ESR analysis of real time radical formation (structurally non-specific) with an ESR flat cell located inside the ESR cavity for magnetic field scans. ESR spectra were recorded with a Bruker EMX spectrometer equipped with a super high Q cavity operating at 9.78 GHz at room temperature. Other ESR spectrometer settings were: magnetic field center, 3494.4 G; magnetic field scan, 70 G; modulation frequency, 100 kHz; microwave power, 20 mW; modulation amplitude, 1.0 G; receiver gain, 5.0×10^4; time constant, 0.655 s; and conversion time, 0.164 s.

On-Line LC/ESR Measurements

After precipitating the COX enzyme and removing ACN as described elsewhere [17-18], the enzyme-free condensed samples were analyzed immediately using on-line LC/ESR and LC/MS for the characterization of POBN adduct structures, or stored at -80°C for later analysis. The online LC/ESR system consisted of an Agilent 1200 series HPLC system and the same Bruker EMX ESR system. The outlet of the Agilent UV detector was connected to a highly sensitive Aquax ESR cell with red PEEK HPLC tubing (0.005 in i.d.). The POBN radical adducts were monitored *via* UV absorption at 265 nm [20-21] followed by ESR detection. There was a delay of about nine seconds between the UV and ESR detection for our on-line ESR settings. LC separations were performed on a C18 column (Zorbax Eclipse-XDB, 4.6×75 mm, 3.5 μm) equilibrated with 90% A (H_2O-0.1% HOAc) and 10% B (ACN-0.1% HOAc). 40 μl of enzyme-free condensed sample was injected into the HPLC system by auto-sampler, and eluted at 0.8 mL/min flow rate with a combination of gradient and isocratic elution: (i) 0-5 min: 90% to 73% of A and 10% to 27% of B; (ii) 5-25 min (isocratic): 73% of A and 27% of B; (iii) 25-40 min: 73% to 30% of A and 27% to 70% of B; (iv) 40-43 min: 30% to 5% of A and 70% to 95% of B; and (v) 43-50 min (isocratic): 5% of A and 95% of B. On-line ESR measurements were performed using a time scan mode with the magnetic field (~3498 G) fixed on the maximum of the first line of the six-line spectrum of the POBN adduct. Other ESR settings were: modulation frequency, 100 kHz; modulation amplitude, 3.0 G; microwave power, 20 mW; receiver gain, 4×10^5; and time constant, 2.6 s.

On-Line LC/MS and LC/MS^2 Measurements

The LC/MS system consisted of an Agilent 1200 series HPLC system and an Agilent Ion Trap SL Mass Spectrometer. The outlet of the UV detector in LC was connected to the MS system with red PEEK HPLC tubing. Chromatographic conditions were identical to those used for on-line LC/ESR. However, the LC flow rate (0.8 mL/min) was adjusted to 30~40 μL/min *via* a splitter directing to the MS inlet. There was a delay of ~35s between the UV and the MS detection for our on-line LC/MS settings. Electrospray ionization (ESI) in positive mode was used for all LC/MS and LC/MS^2 measurements unless otherwise specified. Total ion current (TIC) chromatograms in full mass scan mode (m/z 50 to m/z 600) were performed to profile all products formed in the reaction of COX-catalyzed AA *in vitro* in the presence of POBN. Other MS settings were: capillary voltage, -4500 V; nebulizer press, 20 psi; dry gas flow rate, 8 L/min; dry temperature, 60°C; compound stability, 20%; and number of scans, 50. Extracted ion current (EIC) chromatograms of ions of interest were projected from TIC to acquire MS chromatograms that could match well with ESR chromatograms, where all POBN radical adducts were monitored as ESR-active peaks (structure non-specific). EIC was also performed to determine the number of isomers of given ions. Normally an isolation width of ±0.5 Da was selected for EICs. The multiple reaction monitoring (MRM) mode of LC/MS^2 was conducted to confirm structural assignments of POBN adducts. A width of ±2.0 Da was typically selected to isolate parent ions of interest. Other LC/MS settings were: capillary voltage, -4500 V; nebulizer press, 20 psi; dry gas follow rate, 8 L/min; dry temperature, 60°C; compound stability, 20%; and number of scans, 5.

GC/MS Measurement

GC/MS was used to measure non-free radical products formed from (β-scission of PGF_2-type alkoxyl radicals during COX-catalyzed AA peroxidation. About 200 μl of the *in vitro* reaction mixture was mixed with a total of 3 ml ethyl ether (in three repeated extractions). The ethyl ether layers were then collected, evaporated (by purging with N_2), and resuspended in methanol for GC/MS analysis. The GC/MS system consisted of an HP 6890 GC system equipped with a 5973 Mass Selective Detector. The separation was performed on a DB-5ms column (30m × 0.25 mm × 0.5 μm) with helium as the carrier gas under a constant flow (11.87 psi), inlet temperature (250°C), and temperature program (40°C for 5 min, then increase to 300°C at a rate of 20°C/min). MS detector settings were: MS transfer line heater, thermal AUX 2 temperature 250°C; scan range 10-200; threshold 150; MS source 230°C; MS Quad 150°C; energy 70eV.

Results

Off-Line ESR Study of POBN Trapped Radicals (Structurally Non-Specific)

Maintaining COX enzyme activity during COX-mediated peroxidation *in vitro* requires a reducing agent; one of the most common is phenol [22]. In our experiments, however, we used a stronger reductant, hydroquinone [23], to maintain a higher COX activity, which increased the ESR intensity about 3-4-fold compared to that observed with phenol (unpublished data). For the complete COX-catalyzed AA reaction system using hydroquinone, off-line ESR gave a mixed spectrum composed of a six-line ESR signal of POBN radical adducts ($a^N \approx 15.63$ G and $a^H \approx 2.53$ G) and a five-line ESR signal in the middle from benzosemiquinone radicals generated from hydroquinone oxidation (Figure 1A).

In a control experiment in the absence of POBN (Figure 1B), a five-line spectrum was detected as an ESR signal of benzosemiquinone radical ($a^H \approx 2.35$ G) consistent with that in Figure 1A and published research [24]. In the experiment excluding COX enzyme (Figure 1C), a combination of five- and six-line ESR signals was detected, but at much lower intensity than for the complete system (Figure 1A). This low-intensity spectrum contained benzosemiquinone

radicals and AA-derived, POBN-trapped radicals from autoxidation initiated by iron metals (from hematin). In the absence of AA (Figure 1D), the five-line signal of benzosemiquinone radicals dominated a low-intensity six-line POBN adduct signal ($a^N \approx 15.65$ G and $a^H \approx 2.75$ G). This six-line ESR signal was different from the six-line spectrum of the complete system, and arose from POBN-trapped α-hydroxyethyl radical ($^{\bullet}CH(OH)CH_3$) [15-18] from ethanol oxidation (1% ethanol present in the reaction system excluding AA). In the control experiments excluding either hematin (COX co-factor) or hydroquinone, only about 15%-20% of the intensity of the six-line ESR signal of Figure 1A was observed (data not shown). Thus, the spin trap technique facilitated off-line ESR detection of short-lived radicals, *e.g.* COX-catalyzed and AA-derived free radicals. However, off-line ESR measurement can provide only an overall signal intensity of radical adducts, not specific information in term of types, numbers, and structures since many of the POBN spin adducts tend to have the same or similar hyperfine couplings [25].

LC/ESR and LC/MS Study of POBN Trapped Radicals (Structurally Specific)

In order to obtain more specific radical information from COX-catalyzed AA peroxidation in the presence of POBN, the enzyme-free condensed sample was prepared and subjected to online LC/ESR and LC/MS analysis [15-18]; a UV chromatogram (absorption 265 nm, Figure 2A) and an ESR chromatogram (fixed magnetic field 3498 G on the first line of POBN adduct, Figure 2B) were obtained. Among a total of sixteen ESR-active peaks, many of them could be matched with their corresponding UV peaks (Figures 2A-2B, marked with retention times, t_Rs). The good LC separation made three main types of POBN adducts with numerous isomers readily recognizable from the full scan LC/MS or total ion current chromatogram (TIC, m/z 50-m/z 600, unpublished data): 1) m/z 296 as ESR peaks 5 and 9; 2) m/z 448 as ESR peaks 4, 6, and 13; and 3) m/z 548 as ESR peaks 2-3, 7-8, 10-12, and 14-16.

When the extracted ion current (EIC) chromatograms of m/z 296, m/z 448, and m/z 548 were projected from the TIC, a profile similar to the ESR chromatogram (Figure 2B) was obtained as shown in Figure 2C. Unlike the two abundant MS peaks of the m/z 296 molecule observed in Figure 2C, isomers of other adduct molecules (particularly m/z 548) showed much lower MS abundances compared to their corresponding ESR and UV peaks. These lower detection efficiencies suggest that they might have unique structures that constrain their protonation or low stabilities during MS ionization.

A D_9-POBN spin trapping experiment gave LC/ESR and LC/MS profiles similar to those from POBN, except for slightly shorter retention times and the obligatory 9-Da difference for each corresponding radical adduct [17-18]. The results of the D_9-POBN experiment confirmed the assignment of m/z 296, m/z 448, and m/z 548 ions to spin trapped radicals, and also excluded artifactual ions that might otherwise have been assigned to radical-related products. For any given carbon-centered radical, the number of isomers could be estimated from their individual EIC chromatograms of POBN experiments (Figures 3A, 3C, and 3E), and confirmed if their corresponding isomers were also observed in EIC with a 9-Da difference from D_9-POBN experiments (Figures 3B, 3D, and 3F). The presence of two isomers of the m/z 305 adduct molecule ($t_R \approx$11.8 and 16.9 min, Figure 3C) in the D_9-POBN experiment confirmed that two m/z 296 peaks ($t_R \approx$ 11.9 and 17.3 min, Figure 3B) were the spin adducts of ESR-active peaks 5 and 9, and also excluded two false m/z 296 peaks (labeled 'X') from the tally of radical related products in the POBN experiment. The m/z 457 adduct molecules ($t_R \approx$ 11.5, 14.1, 18.2, 21.2, and 22.2 min) in the D_9-POBN experiment confirmed a total of five isomers of m/z 448 ($t_R \approx$ 11.6, 14.4, 18.4, 22.2, and 23.1 min) as the spin adducts of ESR-active peaks 4, 6, 10, and 12-13, and excluded a false m/z 448 peak (labeled 'X') in the POBN experiment (Figures 3C-3D). Similarly, the m/z 557 peaks in the D_9-POBN experiment confirmed a total of 12 isomers of m/z 548 in the POBN experiment (Figures 3E-3F). Among these 12 isomers,

however, three of them co-eluted with the m/z 296 ion ($t_R \approx 11.9$ min) and two m/z 448 ions ($t_R \approx 18.4$, and 22.2 min), corresponding to ESR-active peaks 5, 10, and 12 respectively.

LC/MS^2 Characterization of POBN Radical Adducts

Since ethanol was used to prepare the AA stock solution, one ESR-active peak (the first, $t_R \approx$ 3.5 min, Figure 2B) corresponded to formation of the POBN-trapped α-hydroxyethyl radical ($^{\bullet}CH(OH)CH_3$) from oxidation of ethanol. This is a radical not related to AA, and LC/MS^2 of its m/z 240 (date not shown) confirmed the structural assignment from its fragment pattern, which agreed with the pattern of POBN/$^{\bullet}CH(OH)CH_3$ published previously [15-18].

Among the three main POBN adducts of AA-derived radicals observed here, the m/z 548 molecule has the largest size and also the greatest number of isomers, which corresponded to a total of 12 ESR-active peaks (Figures 2B and 3E). They were likely the isomers of spin-trapped radicals (POBN/$^{\bullet}C_{20}H_{34}O_5$) formed from rearrangement of PGF_2-type alkoxyl radicals as proposed in Scheme 1-A. However, the low abundance of m/z 548 in LC/MS (positive ion mode) also resulted in a poor quality LC/MS^2 as shown in Figure 4A; even the LC/MS^2 of m/z 557 from the D_9-POBN experiment could not provide enough information (Figure 4B) to support the proposed structure. We believe that this low ESI-MS efficiency of m/z 548 results from the presence of the PGF ring in the vicinity of the protonation site(s) of POBN.

In order to gain better structural information, LC/MS^2 analyses of these isomers were also conducted under negative ion mode. In this mode the same fragment pattern was exhibited in much higher quality LC/MS^2 spectra of POBN/$^{\bullet}C_{20}H_{34}O_5$ (m/z 546, Figure 4C) and D_9-POBN/$^{\bullet}C_{20}H_{34}O_5$ (m/z 555, Figure 4D), *e.g.* ions *a*, *b*, *c*, and *d vs.* ions *a′*, *b′*, *c′*, and *d′* (POBN-related adducts *vs.* D_9-POBN-related adducts [15-18]), confirming this adduct assignment. Indeed, we observed two unique fragmentations: 1) formation of an m/z 289 ion from the POBN experiment and an m/z 298 ion from the D_9-POBN experiment; and 2) formation of an m/z 445 ion from the POBN experiment and an m/z 454 ion from the D_9-POBN experiment (all bold in Figures 4C-4D), suggesting the trapping position of this spin adduct as labeled in Scheme 1-A.

The second type of AA radical-derived spin adduct (m/z 448) formed in COX peroxidation had a total of five isomers as shown in Figures 3C-3D. It appeared to be a POBN-trapped radical derived from β-scission of PGF_2-type alkoxyl radicals, considering that its mass was smaller than m/z 548. The structure and mechanism of formation of m/z 448 (POBN/$^{\bullet}C_{14}H_{21}O_4$) are proposed in Scheme 1-B. The assignment was supported by the agreement between the LC/MS^2 fragment patterns from m/z 448 in the POBN spin trapping experiment (Figure 5A) and m/z 457 in the D_9-POBN spin trapping experiment (Figure 5B).

According to the proposed structure, the spin-trapped radical of m/z 448 has its unpaired electron associated with the carbons of the carbon-carbon double bond nearest the PGF ring following the β-scission as labeled ‘β’’ in Scheme 1-B. This type of (β-scission (toward the C=C) has never been observed in PUFA peroxidation catalyzed by LOX, where the β-scission occurs away from the double bond [15-18]. In order to further confirm this pathway, the POBN spin trapping experiment was also conducted using AA-D_8 (all olefinic hydrogens in AA were replaced by deuterium) as the COX substrate. Two fragment ions of m/z 343 and m/z 361 were observed in the LC/MS^2 analysis of m/z 448 (bold in Figure 5A) in the AA experiment, and their corresponding ions of m/z 350 and m/z 368 were seen in the LC/MS^2 analysis of m/z 455 (POBN/$^{\bullet}C_{14}H_{14}D_7O_4$) in the AA-$D_8$ experiment (bold in Figure 5C), suggesting that one D from AA-D_8 was removed during β-scission as proposed in Scheme 1-B. In other words, this special (β′-scission preferentially occurred toward the carbon-carbon double bond, resulting in removal of the H of AA (or the deuterium of AA-D_8) from the carbon (ω-6) bearing oxygen.

Similar to the EIC of the corresponding m/z 448 ion in the AA system (Figure 3C), five isomers of m/z 455 from AA-D_8 with slight retention time differences were also observed (Inset of Figure 5C), further confirming the structural assignment.

There are only two isomers of the third POBN adduct (m/z 296). This small molecule of m/z 296 appeared to be formed from fragmentation, like the β-scission of a PGF-type alkoxyl radical. In addition to radical products, there is typically a non-radical product from β-scission. Thus, the m/z 296 molecules might be the POBN adducts of secondary radicals that could be generated from the reaction of a non-radical product of β-scission. For the pathway labeled 'β'' in Scheme 1-B, the non-radical product hexanal might be expected, since carbon-centered radicals and aldehydes are two well-known β-scission products. To determine whether hexanal forms from β-scission and whether the POBN adduct of m/z 296 is derived from a hexanal reaction, we also conducted GC experiments to monitor formation of hexanal and ESR spin trapping experiments to monitor m/z 296 ions from a possible free radical reaction of hexanal. Surprisingly, m/z 296 ions were not detected when AA was replaced by hexanal in the COX-reaction system in the presence of POBN nor was hexanal detected from the complete reaction system (data not shown).

We therefore propose that perhaps due to the strong reducing and liquid phase environment, a non-radical product alcohol (hexanol) could form by a proposed mechanism (Scheme 1-B) instead of forming aldehyde. In fact, formation of 1-hexanol was confirmed by the GC experiments from our reaction system. Formation of two identical isomers of the POBN adduct of the 1-hydroxyhexyl radical were also observed when AA was replaced by 1-hexanol in the COX reaction system as well as when Fenton reagents (or ferrous iron alone) reacted with 1-hexanol in the presence of POBN (unpublished data). Furthermore, observation of the same fragment pattern for different ions (*c* ions: m/z 196 *vs.* m/z 205; *c*-O ions: m/z 179 *vs.* m/z 188; *b* ions: m/z 209 *vs.* m/z 210; *b*-C_5H_{11}: m/z 138 *vs.* m/z 139; and *b*-$C_7H_{14}O$ *vs. b*-$C_7H_{13}DO$ ion: m/z 96) in the LC/MS^2 of m/z 296 (Figure 6A) from the POBN spin trapping experiment with AA, the LC/MS^2 of m/z 305 (Figure 6B) from the D_9-POBN spin trapping experiment with AA, and the LC/MS^2 of m/z 297 (Figure 6C) from the POBN spin trapping experiment with AA-D_8 conclusively confirmed its structural assignment.

There is also another type of β-scission (labeled as 'β'in Scheme 1-B) [15-18] that takes place to form a radical ($^{\bullet}C_5H_9$) trapped as the POBN adduct of the m/z 266 ion. A small amount of m/z 266 was actually measured as the third component of the ESR-active peak 13 at $t_R \approx 23.1$ min (m/z 448 and m/z 548 were the others).

Characterization of POBN Radical Adducts Formed from Cellular Peroxidation

Although the POBN spin trapping technique has been successfully used to measure free radicals formed from cellular peroxidation in many studies [26], the structures of these adducts have never been characterized. Here for the first time, we have used a combination of ESR spin trapping, LC/ESR, and LC/MS to characterize in detail the structures of POBN adducts formed from PC-3 cellular peroxidation.

When the PC-3 cells were not supplemented with AA, peroxidation in the presence of POBN yield no ESR six-line signal from POBN adducts in off-line ESR under our experimental conditions. However, when PC-3 cells were incubated with both AA and POBN, a typical six-line signal of POBN adduct ($a^N \approx 15.72$ G and $a^H \approx 2.55$ G, Figure 7A) was observed. A reliable LC/ESR profile of the experiment in Figure 7B (after the analyte was processed with enzyme denaturation, supernatant collection, and sample condensation, see Materials and Methods) could not be obtained from the cellular experiment due to the relative lower sensitivity of on-line ESR measurement. However, formation of 1-hydroxyhexyl radicals during PC-3 cell peroxidation was supported by the observation of two EIC m/z 296 peaks at $t_R \approx 11.9$ and 17.3

min as POBN/$^{\bullet}C_6H_{13}O$ (Figures 7B) from the POBN experiment. In addition, two isomers in each EIC of m/z 305 and m/z 297 were also observed (Figures 7C-7D) from D_9-POBN and AA-D_8/POBN experiments. The LC/MS^2 analysis of these molecules demonstrated a fragmentation pattern identical to those of Figure 6 (data not shown), further confirming that PC-3 cellular peroxidation metabolizes AA as in the proposed COX-mechanism (Scheme 1) *via* a novel β-scission.

Discussion

In COX-catalyzed arachidonic acid (AA) peroxidation, a reducing co-substrate is needed to maintain cyclooxyenase activity. We have tested three different reducing co-substrates that have similar structures and known roles in the COX reaction [23]: hydroquinone, acetaminophen, and phenol. In our study, generation of POBN adducts with these co-substrates, reflecting COX activity, showed a good correlation with their reported reducing abilities in the order hydroquinone > acetaminophen > phenol (data not shown). In addition, there were no radical adducts other than m/z 548, m/z 448, m/z 296, and m/z 266 observed in any of the three systems, suggesting similar roles for the three agents in maintaining COX activity. We selected the COX peroxidation reaction with hydroquinone for our LC/ESR/MS study because it formed the most abundant radical adducts, especially the m/z 548 isomers.

COX-catalyzed AA peroxidation *in vitro* in the presence of POBN yielded four types of free radical adducts (m/z 548, m/z 448, m/z 296, and m/z 266) as shown in Scheme 1A-B. When some LC/MS^2 spectra exhibited low quality during the POBN spin trapping experiment, perhaps due to low ionization efficiency or low stability of certain types of radical adduct, we conducted two more different spin-trapping experiments to ensure our assignment of adduct structure: 1) D_9-POBN spin trapping, in which POBN was replaced with the same amount of D_9-POBN, and the same types of fragmentation were then screened for either the same MS ions or those with a 9-Da difference (Figures 4-6) [27-28]; and 2) AA-D_8 peroxidation, in which AA was replaced by AA-D_8 as a substrate of COX, and then the MS ions from both peroxidation systems were analyzed and compared to determine the exact structures of β-scission products (Figures 5-7). Unlike the gradient elution using a semi-aqueous mobile phase where consistent retention differences were observed for all corresponding POBN and D_9-POBN trapped free radicals [17], the retention time differences of corresponding spin trapped radicals were inconsistent under our elution conditions (a combination of gradient and isocratic elutions, see Materials and Methods). The differences were more extensive during isocratic elution (5-25 min) than gradient [17]. In general, the more hydrophobic the radicals, the greater the observed difference of retention time between POBN and D_9-POBN adducts (Figure 3).

Similar ionization efficiencies have been reported for POBN-trapped PUFA-derived radicals formed from LOX-mediated peroxidation [17-18]. The POBN adducts of m/z 448 (POBN/$^{\bullet}C_{14}H_{21}O_4$) and m/z 548 (POBN/$^{\bullet}C_{20}H_{34}O_5$) were actually the first two adduct molecules that showed very low MS efficiencies compared to their ESR and UV detection during on-line separation. Their low MS efficiencies most likely resulted from the steric hindrance of protonation of the POBN adduct from the vicinity of the PGF ring or their low stabilities during MS ionization.

Due to its hydrophilic nature, the concentration of POBN accessible to the cellular radical generation site (inside the cell membrane) was very limited. Only < 2% of the POBN was estimated to be able to pass the cell membrane under our experimental conditions (unpublished data). Thus, it was not surprising that the radicals $^{\bullet}C_{20}H_{34}O_5$ and $^{\bullet}C_{14}H_{21}O_4$ were able to form inside the cells, but the production of their adduct forms was very limited and their corresponding MS peaks of m/z 548 and m/z 448 were unable to be detected. In our cell system, only the m/z 296 adduct ($^{\bullet}C_6H_{13}O$) was measured (Figure 7C) because of its much higher MS

efficiency. Indeed, considering the different pathways forming m/z 296, m/z 548, and m/z 448 molecules (Scheme 1), measurement of the m/z 296 ion as a POBN adduct of 1-hydroxyhexyl in cells could have a great advantage in intensity since its precursor could be a non-radical product (hexanol, Scheme 1-B). Hexanol could form and be released readily from cells, and its secondary free radical oxidation could occur anywhere if a trace of the metal iron is available. In our cell system, spin trapped 1-hydroxyhexyl radicals originated mainly from hexanol oxidation in the cell medium, where a higher concentration of POBN was available to trap them for off-line ESR and LC/MS analysis. Observations of similar off-line ESR intensity from cells-PBS suspensions and cells-free PBS support this proposal (unpublished data).

There were two proposed pathways for the formation of the m/z 548 adduct (POBN/$^{\bullet}C_{20}H_{34}O_5$) as described in Scheme 1-A: 1) PGG_2 is converted to PGH_2, the radical is trapped, and then the dioxygen bridge of the PGH2-type radical is reduced; and 2) the dioxygen bridge of PGG_2 is reduced *via* the formation of 15-hydroperoxy-PGF_2 (15-OOH PGF_2, Reaction 2), subsequent reactions convert 15-OOH PGF_2 to form a PGF_2-type carbon-centered radical, and the radical is trapped by POBN. Isomers of m/z 548 might also result from the spin trapping of the carbon-centered radical intermediate (POBN/$^{\bullet}C_{20}H_{34}O_5$) as proposed in Scheme 1-B (1, 5 intra-molecular H abstraction). Since PGH_2-type radicals were not detected in our study, the second pathway appears to be more reasonable. In other words, 15-OOH PGF_2 might also form *via* a pathway other than a non-Se-hGPx enzymatic reaction [29]. It might play an important role yet to be defined in terms of free radical formation in COX biology.

The inventory and characterization of free radicals presented in this study, particularly the radicals formed from a special β′ scission, including the C=C centered radicals and α-hydroxyhexyl radicals (Scheme 1B), improves our knowledge of COX-mediated peroxidation. We have observed the special β-scission and novel radical formation from COX-catalyzed AA peroxidation in many human cancer cell lines (unpublished data), and the possible impacts of those radical products in COX biology will be studied in our future research. Two novel products from special β-scission, i.e., the C=C centered free radical (referred to as the m/z 448 ion) and the hydroxyhexyl radical (referred to as the m/z 296 ion) will be particularly investigated due to their special reactivity and unique source (hydroxyhexyl radical can be obtained by oxidation readily from hexanol), in terms of their ability to target bio-molecules inside cells and tissues.

Acknowledgments

This work was supported by NIEHS Grant ES-012978. We also appreciate China Pharmaceutical University's support of part of Mr. Yu's salary.

List of Abbreviations

AA
: Archidonic acid (*all-cis*-5, 8, 11, 14-eicosatetraenoic acid)

COX
: Cyclooxygenase

EIC
: Extracted Ion Current-chromatography

ESR
: Electron Spin Resonance

GC

Gas chromatography

HPLC (LC)

High Performance Liquid Chromatography

MRM

Multiple Reaction Monitoring

MS

Mass Spectroscopy

PGs

Prostaglandins

POBN

α-[4-pyridyl-1-oxide]-N-*tert*-butyl nitrone

TIC

Total Ion Current-chromatography

t_R

Retention time

References

1. Smith WL, DeWitt DL, Garavito RM. CYCLOOXYGENASES: Structural, Cellular, and Molecular Biology. Annu Rev Biochem 2000;69:145–182. [PubMed: 10966456]
2. Dubois RN, Tsujii M, Bishop P, Awad JA, Makita K, Lanahan A. Cloning and characterization of a growth factor-inducible cyclooxygenase gene from rat intestinal epithelial cells. Am J Physiol (Gastrointest Liver Physiol) 1994;266:G822–G827.
3. Jones DA, Carlton DP, McIntyre TM, Zimmerman GA, Prescott SM. Molecular Cloning of Human Prostaglandin Endoperoxide Synthase Type II and Demonstration of Expression in Response to Cytokines. J Biol Chem 1993;268:9049–9054. [PubMed: 8473346]
4. Buskens CJ, van Rees BP, Sivula A, Reitsma JB, Haglund C, Bosma PJ, Offerhaus GJA, van Lanschot JJB, Ristimaki A. Prognostic significance of elevated cyclooxygenase 2 expression in patients with adenocarcinoma of the esophagus. Gastroenterology 2002;122:1800–1807. [PubMed: 12055587]
5. Sano H, Kawahito Y, Wilder RL, Hashiramoto A, Mukai S, Asai K, Kimura S, Kato H, Kondo M, Hla T. Expression of Cyclooxygenase-1 and -2 in Human Colorectal Cancer. Cancer Res 1995;55:3785–3789. [PubMed: 7641194]
6. Wolff H, Saukkonen K, Anttila S, Antti K, Harri V, Ristimaki A. Expression of cyclooxygenase-1 in human lung carcinoma. Cancer Res 1998;58:4997–5001. [PubMed: 9823297]
7. Sales KD, Katz AA, Davis M, Hinz S, Soeters RP, Hofmeyr MD, Millar RP, Jabbour HN. Cyclooxygenase-2 expression and prostaglandin E_2 synthesis are up-regulated in carcinomas of the cervix: a possible autocrine/paracrine regulation of neoplastic cell function via EP2/EP4 receptor. J Clin Endocrinol Metab 2001;86:2243–2249. [PubMed: 11344234]
8. Lee LM, Pan CC, Cheng CJ, Chi CW, Liu TY. Expression of cyclooxygenase-2 in prostate adenocarcinoma and benign prostatic hyperplasia. Anticancer Res 2001;21:1291–1294. [PubMed: 11396201]
9. Marnett LJ, Rowlinson SW, Goodwin DC, Kalgutkar AS, Lanzo CA. Arachidonic Acid Oxygenation by COX-1 and COX-2. J Biol Chem 1999;274:22903–22906. [PubMed: 10438452]
10. Ohki S, Ogino N, Yamamoto S, Hayaishi O. Prostaglandin Hydroperoxidase, an Integral Part of Prostaglandin Endoperoxide Synthetase from Bovine Vesicular Gland Microsomes. J Biol Chem 1979;254:829–836. [PubMed: 104998]
11. Lu G, Tsai AL, Van Wart HE, Kulmacz RJ. Comparison of the Peroxidase Reaction Kinetics of Prostaglandin H Synthase-1 and -2. J Biol Chem 1999;274:16162–16167. [PubMed: 10347169]

12. Hemler ME, Lands WEM. Evidence for a Peroxide-initiated Free Radical Mechanism of Prostaglandin Biosynthesis. J Biol Chem 1980;255:6253–6261. [PubMed: 6771268]
13. Jiang J, Borisenko GG, Osipov A, Martin I, Chen R, Shvedova AA, Sorokin A, Tyurina YY, Potapovich A, Tyurin VA, Graham SH, Kagan VE. Arachidonic acid-induced carbon-centered radicals and phospholipid peroxidation in cyclo-oxygenase-2-transfected PC12 cells. J Neurochem 2004;90:1036–1049. [PubMed: 15312159]
14. Schreiber J, Eling TE, Mason RP. The oxidation of arachidonic acid by the cyclooxygenase activity of purified prostaglandin H synthase: spin trapping of a carbon-centered free radical intermediate. Arch Biochem Biophys 1986;249:126–136. [PubMed: 3017218]
15. Qian SY, Yue GH, Tomer KB, Mason RP. Identification of All Class of Spin-trapped Carbon-centered Radicals in Soybean Lipoxygenase-dependent Lipid Peroxidation of ω-6 Polyunsaturated Fatty Acids *via* LC/ESR, LC/MS, and Tandem MS. Free Radic Biol Med 2003;34:1017–1028. [PubMed: 12684086]
16. Qian SY, Guo Q, Mason RP. Identification of Spin Trapped Carbon-Centered Radicals in Soybean Lipoxygenase-Dependent Peroxidation of ω-3 Polyunsaturated Fatty Acids by LC/ESR, LC/MS, and Tandem MS. Free Radic Biol Med 2003;35:33–44. [PubMed: 12826254]
17. Yu Q, Shan Z, Ni K, Qian SY. LC/ESR/MS Study of Spin Trapped Carbon-Centered Radicals Formed From *in vitro* Lipoxygenase-Catalyzed Peroxidation of γ-Linolenic Acid. Free Radic Res 2008;42:442–455. [PubMed: 18484409]
18. Shan Z, Yu Q, Purwaha P, Guo B, Qian SY. A combination study of spin-trapping, LC/ESR and LC/MS on carbon-centred radicals formed from lipoxygenase-catalysed peroxidation of eicosapentaenoic acid. Free Radic Res 2009;43:1–15. [PubMed: 19598034]
19. Buettner GR. In the absence of catalytic metals ascorbate does not autoxidize at pH 7: ascorbate as a test for catalytic metals. J Biochem Biophys Methods 1988;16:27–40. [PubMed: 3135299]
20. Albro PW, Knecht KT, Schroeder JL, Corbett JT, Marbury D, Collins BJ, Charles J. Isolation and characterization of the initial radical adduct formed from linoleic acid and α-(4-pyridyl-1-oxide)-N-tert-butylnitrone in the presence of soybean lipoxygenase. Chem Biol Interact 1992;82:73–89. [PubMed: 1312396]
21. Ortiz de Montellanto PR, Augusto O, Viola F, Kunze KL. Carbon radicals in the metabolism of alkyl hydrazines. J Biol Chem 1983;258:8623. [PubMed: 6305994]
22. Hsuanyu Y, Dunford HB. Prostaglandin H Synthase Kinetics. The Effect of Substituted Phenols on Cyclooxygenase Activity and the Substituent effect on Phenolic Peroxidatic Activity. J Biol Chem 1992;267:17649–17657. [PubMed: 1517213]
23. Markey CM, Alward A, Weller PE, Marnett LJ. Quantitative Studies of Hydroperoxide Reduction by Prostaglandin H Synthase. Reducing Substrate Specificity and the Relationship of Peroxidase to Cyclooxygenase Activities. J Biol Chem 1987;262:6266–6279. [PubMed: 3106353]
24. Rao DNR, Takahashi N, Mason RP. Characterization of a Glutathione Conjugate of the 1,4-Benzosemiquinone-free Radical Formed in Rat Hepatocytes. J Biol Chem 1988;263:17981–11786. [PubMed: 2848019]
25. Buettner GR. Spin Trapping: EPR parameters of spin adducts. Free Radic Biol Med 1987;3:259–303. [PubMed: 2826304]
26. Qian SY, Wang HP, Schafer FQ, Buettner GR. EPR Detection of Lipid-derived Free Radicals from PUFA, LDL, and Cell Oxidations. Free Radic Biol Med 2000;29:568–579. [PubMed: 11025200]
27. Qian SY, Chen YR, Deterding LJ, Fann YC, Chignell CF, Tomer KB, Mason RP. Identification of protein-derived tyrosyl radical in the reaction of cytochrome c and hydrogen peroxide: characterization by ESR spin-trapping, HPLC and MS. Biochem J 2002;363:281–288. [PubMed: 11931655]
28. Qian SY, Kadiiska MB, Guo Q, Mason RP. A novel protocol to identify and quantify all spin trapped free radicals from *in vitro/in vivo* interaction of $HO^{\bullet}$ and DMSO: LC/ESR, LC/MS, and dual spin trapping combinations. Free Radic Biol Med 2005;38:125–135. [PubMed: 15589381]
29. Hong Y, Li CH, Burgess JR, Chang M, Salem A, Srikumar K, Reddy CC. The Role of Selenium-dependent and Selenium-independent Glutathione Peroxidases in the Formation of Prostaglandin $F_{2\alpha}$. J Bio Chem 1989;264:13793–13800. [PubMed: 2760044]

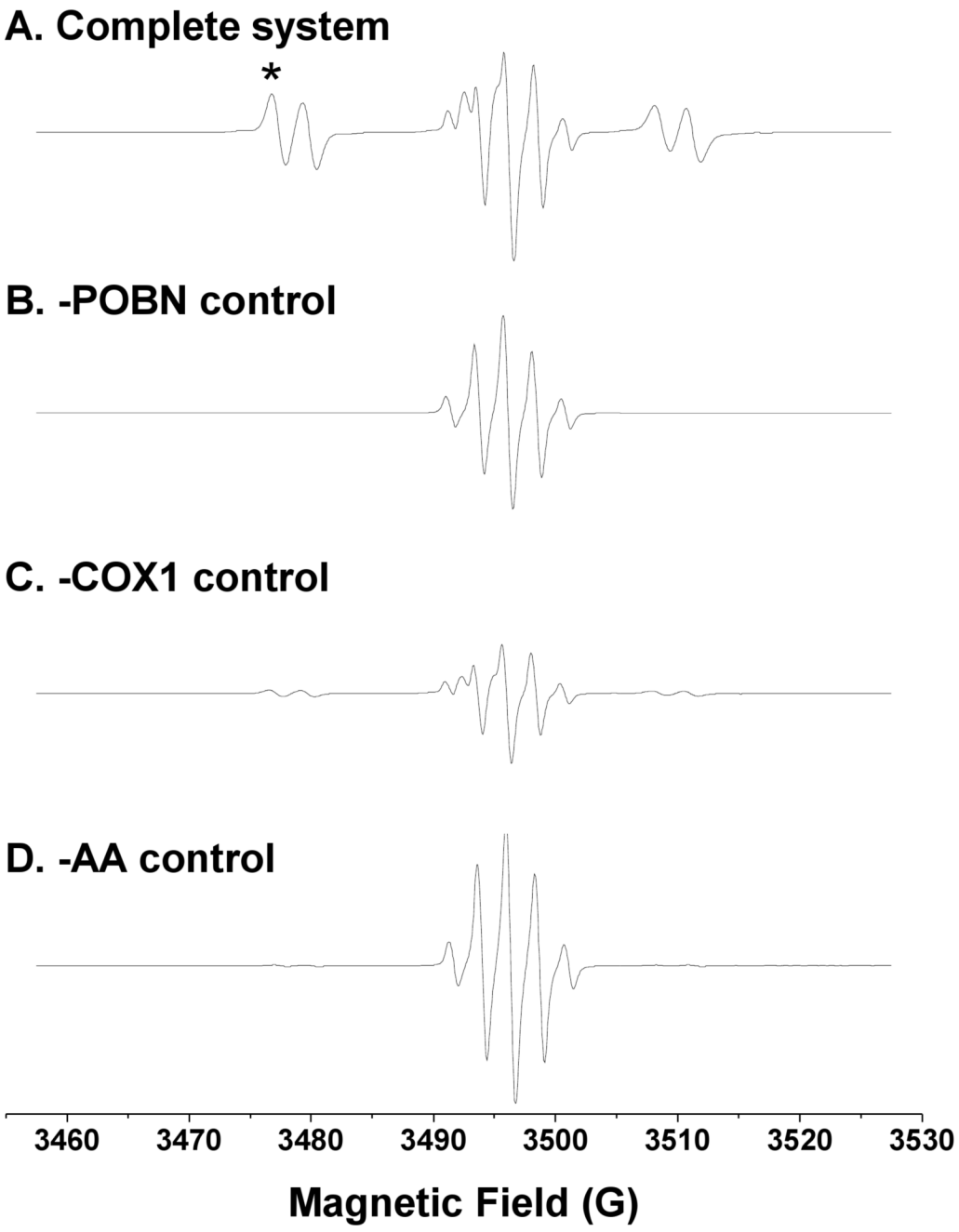

Figure 1.

Off-line ESR spectra from the complete COX-AA reaction system (incubated 30 min) and its relevant controls. (**A**) ESR spectrum of complete reaction system (100 mM Tris-Cl buffer, pH 8.0) containing 100 mM POBN, 50 μM hematin, 5 KUnits/mL COX1 or COX2, 5 mM hydroquinone, and 2 mM AA. A six-line ESR signal ($a^N \approx 15.63$ G, $a^H \approx 2.53$ G) overlapped a five-line signal (benzosemiquinone radicals) at the center of the spectrum; (**B**) ESR spectrum of the reaction excluding POBN. A five-line signal of benzosemiquinone radical was observed ($a^H \approx 2.35$ G); (**C**) ESR spectrum of the reaction excluding COX. A combination of five- and six-line ESR signals was measured at much lower intensities than that of the complete reaction system; and (**D**) ESR spectrum of the reaction excluding AA. A five-line benzosemiquinone

radical signal dominated a very weak six-line ESR signal ($a^N \approx 15.65$ G, $a^H \approx 2.75$ G), which represents the POBN adduct of α-hydroxyethyl radical ($^{\bullet}CH(OH)CH_3$) formed from ethanol oxidation (1% ethanol, *v/v*, present in the system because the AA-ethanol stock solution was replaced by ethanol). Note that magnetic field scans were all centered at 3494.4 G, and the low magnetic field for the first line of the six-line POBN adduct spectrum (marked as '*' in Figure 1A) was fixed and used to monitor radical adducts in on-line LC/ESR measurements (Figure 2). However, the field (~3474 G) for off-line measurements differed slightly from the on-line field in Figure 2 because different ESR cells were used.

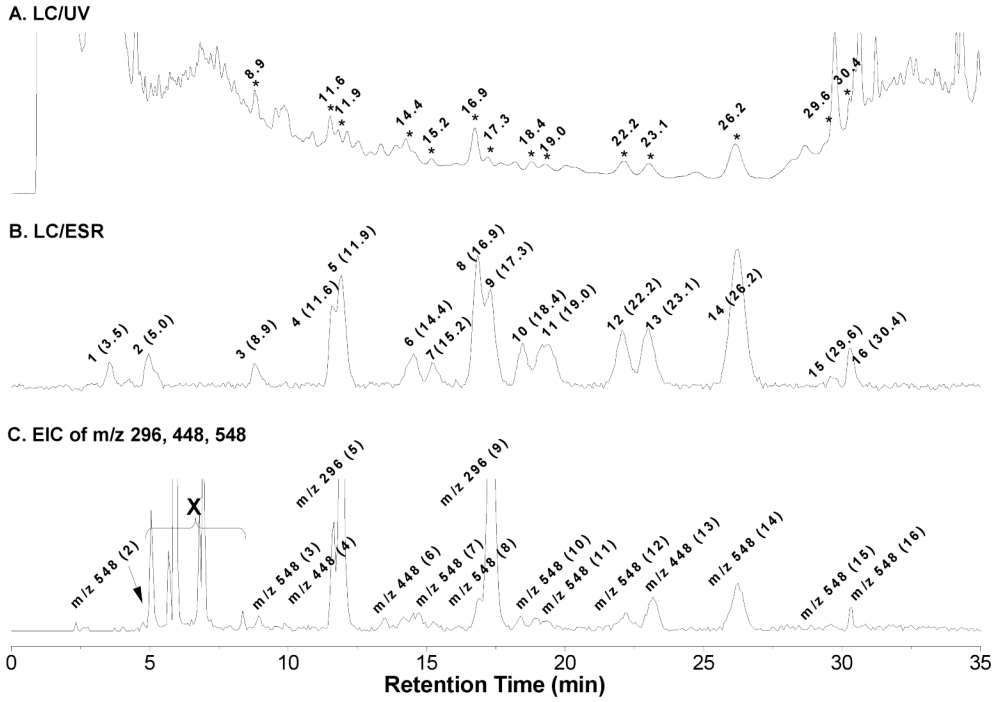

Figure 2.

On-line LC/ESR and LC/MS chromatograms of complete COX-AA reaction system (incubated 30 min). (**A**) UV chromatogram at 265 nm using a C_{18} column and combination of gradient and isocratic elution (details described in Materials and Methods). Peaks of interest are labeled by retention time (min); (**B**) ESR chromatogram with ESR magnetic field fixed on the maximum of the first line of the six-line signal. There was a nine second offset between the UV and the ESR detection due to the connections. All ESR-active peaks are labeled by number as well as the retention time (min); (**C**) Projected EIC of m/z 548, m/z 448, and m/z 296 (from on-line LC/MS, full scan from m/z 50 to m/z 600). There was an offset of thirty-five seconds between the UV and MS measurements due to the connection settings. All MS-active peaks are also labeled with their corresponding ESR-active peaks numbers. Note that the first two minutes of LC eluant always bypassed the MS detector and the peaks on the EIC marked with 'X' were the false peaks. The fixed field on the first line of the POBN adduct was shifted to ~3498 G in on-line LC/ESR from ~3474 G in off-line ESR (asterisked in Figure 1A) due to different resonance frequencies of the flat cell and the Aquax cell.

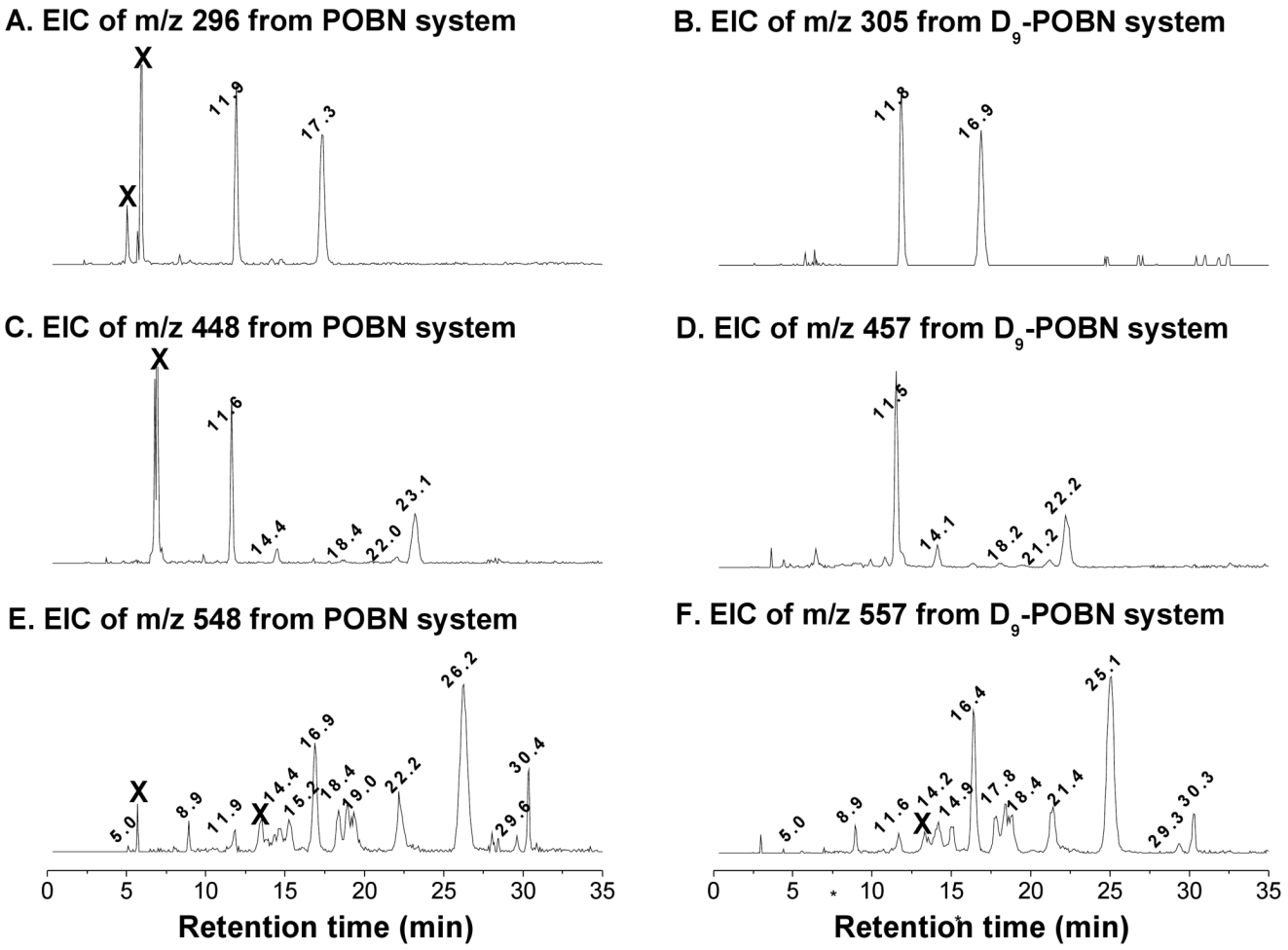

Figure 3.

Individual EIC of complete COX-AA reaction system (incubated 30 min). (**A**-**B**) EICs of m/z 296 and m/z 305 from the POBN and D_9-POBN spin trapping experiments, respectively; (**C**-**D**) EICs of m/z 448 and m/z 457 from the POBN and D_9-POBN spin trapping experiments, respectively; and (**E**-**F**) EICs of m/z 548 and m/z 557 from the POBN and D_9-POBN spin trapping experiments, respectively. The retention time differences between POBN- and D_9-POBN-trapped radicals were inconsistent during isocratic elution (5-25 min). Note that all isomers of each adduct are labeled by their retention times in EICs, while peaks marked by 'X' were the false ions because they are ESR-silent and not confirmed in the D_9-POBN experiments.

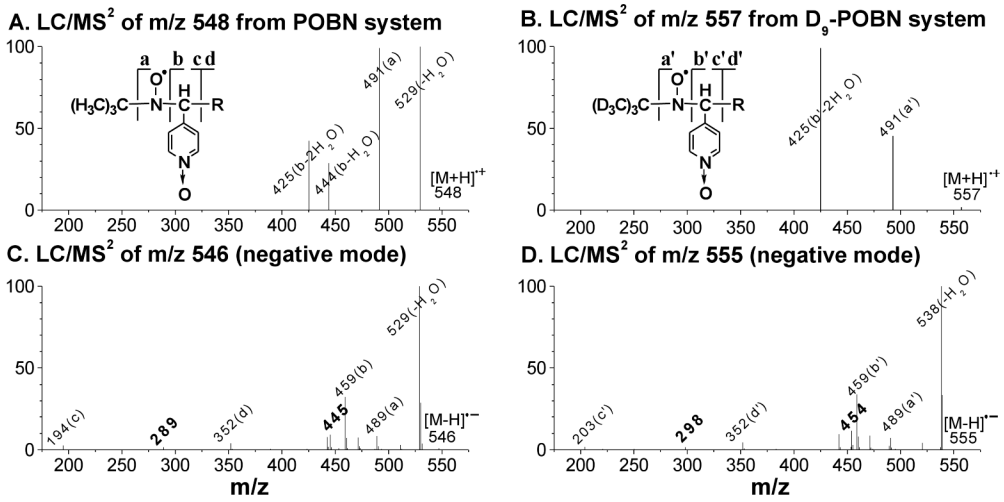

Figure 4.

LC/MS^2 analysis of spin adduct of the $^{\bullet}C_{20}H_{34}O_5$ radical. (**A-B**) LC/MS^2 (positive ion mode) of m/z 548 and m/z 557 from POBN and D_9-POBN spin trapping experiments, respectively; (**C-D**) LC/MS^2 (negative ion mode) of m/z 546 and m/z 555 from POBN and D_9-POBN spin trapping experiments, respectively. Fragment ions of m/z 289 and m/z 445 (bold) in the POBN experiment corresponded to those of m/z 298 and m/z 454 in the D_9-POBN experiment, suggesting the radical trapping site of the spin adduct as described in Scheme 1-A. Note that although the same fragmentation pattern was observed in LC/MS^2 analysis of its 12 isomers, the spectra failed to offer enough information to distinguish differences among the relevant isomers.

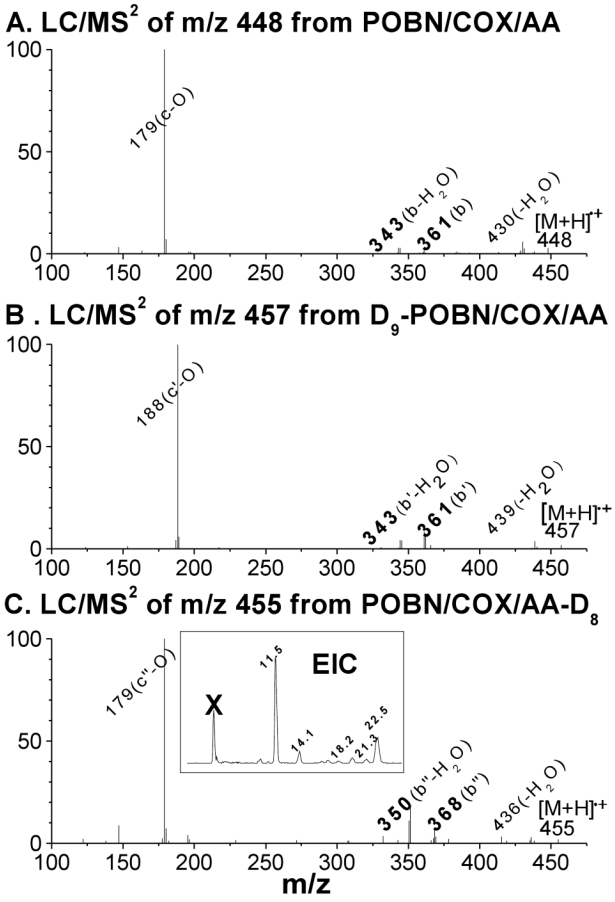

Figure 5.

LC/MS^2 analysis of spin adduct of the $^{\bullet}C_{14}H_{21}O_4$ radical. (**A**) LC/MS^2 of m/z 448 from the COX-AA reaction in the presence of POBN; (**B**) LC/MS^2 of m/z 447 from the COX-AA reaction in the presence of D_9-POBN; (**C**) LC/MS^2 of m/z 455 from the COX-AA-D_8 reaction in the presence of POBN; and (**inset of C**) EIC of m/z 455 from the COX-AA-D_8 reaction in the presence of POBN. Observation of *b* ions as m/z 343 *vs.* m/z 361 and *b*-H_2O ions as m/z 350 *vs.* m/z 368 supported the proposed structure described as a special β-scission preferentially occurring towards the carbon-carbon double bond, resulting in removal of the H of AA (or the deuterium of AA-D_8) from the carbon (ω-6) bearing oxygen (labeled as β′ in Scheme 1-B). Note that although the same fragmentation pattern was observed in all LC/MS^2 analyses of its five isomers, the spectra failed to offer enough information to distinguish their differences.

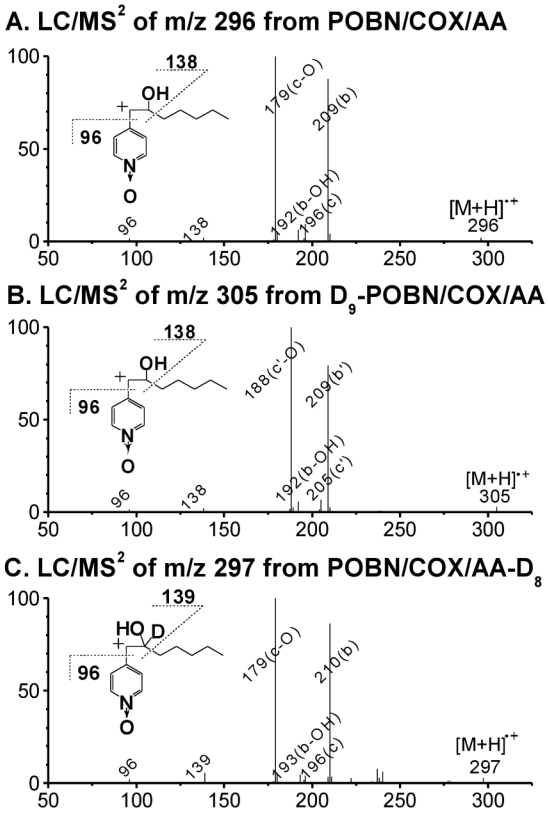

Figure 6.

LC/MS^2 analysis of the spin adduct of the $^{\bullet}C_6H_{12}O$ molecule. (**A**) LC/MS^2 of m/z 296 from the COX-AA reaction in the presence of POBN; (**B**) LC/MS^2 of m/z 305 from the COX-AA reaction in the presence of D_9-POBN; and (**C**) LC/MS^2 of m/z 297 from the COX-AA-D_8 reaction in the presence of POBN. Note that observation of same fragmentation pattern, including those from the inset *b*-ion structures in 3 spin trapping experiments, confirmed the structure assignment. Although the same fragmentation pattern was observed in LC/MS^2 of its two isomers, the spectra failed to offer enough information to distinguish a difference among the relevant isomers.

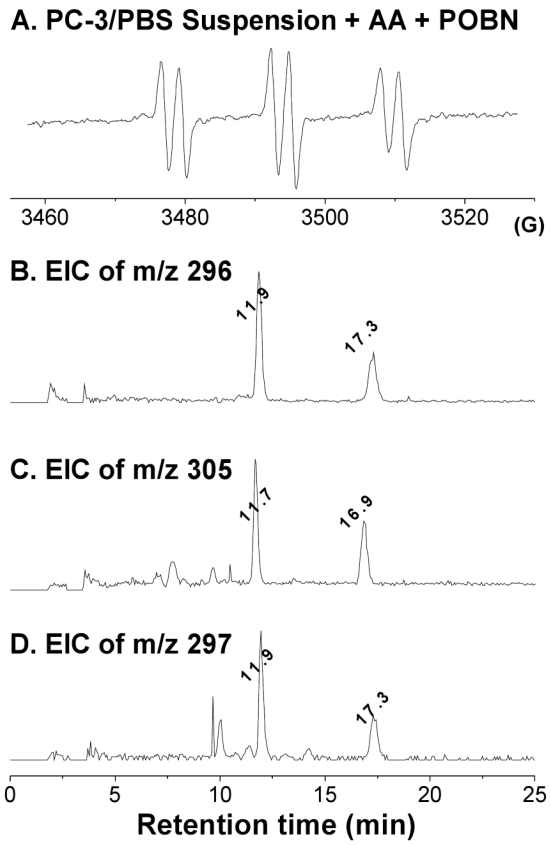

Figure 7.

Off-line ESR and EIC analysis of radicals formed from PC-3 cellular peroxidation. (**A**) off-line ESR study of cell-PBS suspension incubated with 30 mM POBN and 0.5 mM AA for 30 min; (**B-D**) EICs of m/z 296, m/z 305, and m/z 297 projected from the LC/MS^2 of cellular COX-AA peroxidation in the presence of POBN, D_9-POBN, and POBN-AA-D_8, respectively.

Scheme 1-A

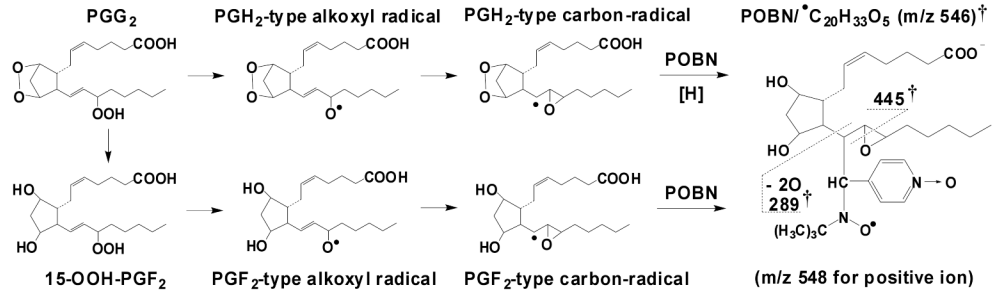

Scheme 1-B

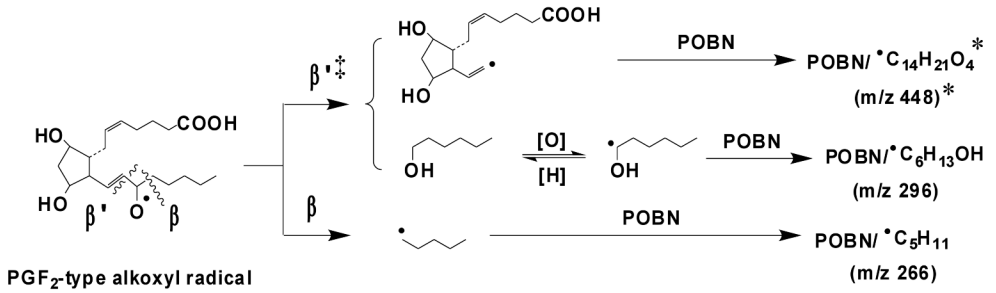

Scheme 1.

Proposed mechanisms of formation of spin trapped free radicals from COX-AA peroxidation. (**A**) Formation of the m/z 548 adduct; (**B**) Formation of m/z 448 and m/z 296.

'†': in the case of the D_9-POBN experiment, two fragment ions of m/z 454 and m/z 298 were measured in the LC/MS^2 (negative ion mode) of m/z 555 (D_9-POBN/$^{\bullet}C_{20}H_{33}O_5$).

'‡': a proposed special β′-scission, *via* 1, 5 intra-molecular H abstraction, to form hexanol and/or hydroxyhexyl radical ($^{\bullet}C_6H_{11}O$), rather than forming hexanal:

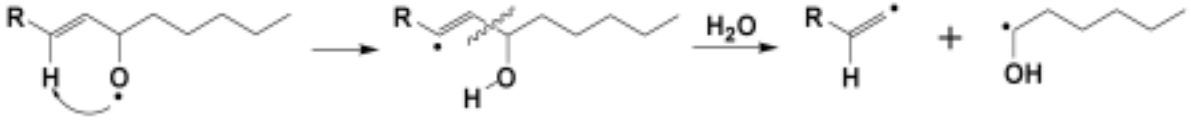

'*': in the case of AA-D_8, formation of the m/z 455 ion as POBN/$^{\bullet}C_{14}H_{14}D_7O_4$ as the deuterium of AA-D_8 (or the H of AA) is removed from the ω-6 carbon:

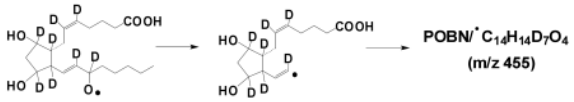

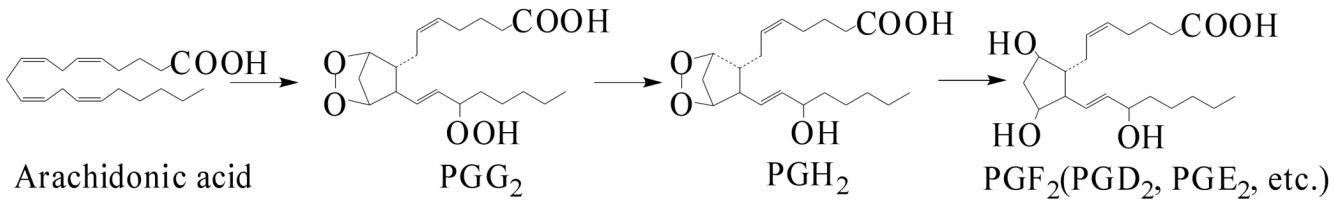

Reaction 1.

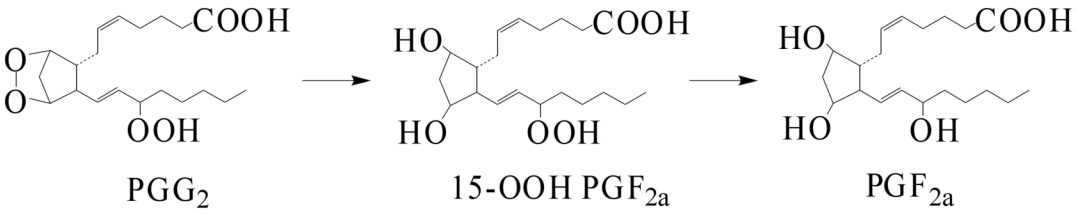

Reaction 2.